Biosensors and Bioelectronics 39 (2013) 282–288

Contents lists available at SciVerse ScienceDirect

Biosensors and Bioelectronics

journal homepage: www.elsevier.com/locate/bios

Impedimetric biosensor based on cell-mediated bioimprinted films for bacterial detection

Peng Qi [a,b], Yi Wan [a,b], Dun Zhang [a,*]

[a] Shandong Provincial Key Laboratory of Corrosion Science, Institute of Oceanology, Chinese Academy of Sciences, 7 Nanhai Road, Qingdao 266071, China
[b] Graduate School of the Chinese Academy of Sciences, 19 (Jia) Yuquan Road, Beijing 100039, China

ARTICLE INFO

Article history:
Received 9 May 2012
Received in revised form
30 July 2012
Accepted 31 July 2012
Available online 9 August 2012

Keywords:
Sulfate-reducing bacteria
Graphene
Electrochemical impedance spectroscopy
Bioimprinted film
Electrodeposition

ABSTRACT

This work presents the synthesis of bacteria-mediated bioimprinted films for selective bacterial detection. Marine pathogen sulfate-reducing bacteria (SRB) were chosen as the template bacteria. Chitosan (CS) doped with reduced graphene sheets (RGSs) was electrodeposited on an indium tin oxide electrode, and the resulting RGSs-CS hybrid film served as a platform for bacterial attachment. The electrodeposition conditions were optimized to obtain RGSs-CS hybrid films with excellent electrochemical performance. A layer of nonconductive CS film was deposited to embed the pathogen, and acetone was used to wash away the bacterial templates. Electrochemical impedance spectroscopy was performed to characterize the stepwise modification process and monitor the SRB population. Faradic impedance measurements revealed that the charge transfer resistance (R_{ct}) increased with increased SRB concentration. A linear relationship between ΔR_{ct} and the logarithm of SRB concentration was obtained within the concentration range of 1.0×10^4 cfu mL^{-1} to 1.0×10^8 cfu mL^{-1}. The impedimetric sensor showed good selectivity towards SRB based on size and shape. Hence, selectivity for bacterial detection can be improved if the bioimprinting technique is combined with other bio-recognition elements.

1. Introduction

Molecularly imprinting technology has a wide range of applications, such as catalysis, separation, purification, drug delivery, and detection (Chen et al., 2011; Haupt and Mosbach, 2000). In most cases, the target substances are subnanometer molecules, including toxic compounds (Syu et al., 2006; Thoelen et al., 2008), amino acids (Li and Husson, 2006; Özcan et al., 2006), sugars (Cheng et al., 2001; Manju et al., 2010) and drugs (Hong et al., 2010; Mazzotta et al., 2008). The imprinting of much larger structures has been hitherto considered greatly challenging. Dickert's group has recently developed a soft lithographic technique to construct quartz crystal microbalance biosensors. The bioimprinted films were formed by 'stamping' the immobilized templates into the surface of a thin polymer layer. The resultant bioimprinted films could selectively detect target virus (Hayden et al., 2006), bacteria (Dickert and Hayden, 2002; Hayden and Dickert, 2001), and cells (Hayden et al., 2003). Bolisay et al. (2006) have synthesized crosslinked polymers imprinted against tobacco mosaic virus (TMV) via covalent interactions. The TMV-imprinted polymer demonstrated preferential selectivity for target virus based on shape differences. The cell-mediated bioimprinting method has first been used by Aherne et al. (1996) to form lithographic imprints of whole yeast cells. The bioimprinted films were synthesized as follows. Poly (amine) and diacid chloride were added to an organic solution containing yeast cells, and then the cells were immobilized at the organic–aqueous interface of the microcapsule via the covalent bonds between poly (amine) and nucleophilic groups in the bacteria. Finally the microcapsule was crosslinked by the photopolymerization of diacrylate. This cell-mediated approach can successfully mimic the shape and size of the real cell. Based on this method, Namvar and Warriner (2007) have imprinted *Bacillus subtilis* endospores with conducting polymer films to detect the endospores either directly by monitoring changes in the electrochemistry of the conducting polymer film or indirectly by following the germination of bound endospores. The imprinted films were synthesized by absorbing endospores on the surface of glassy carbon electrodes, and a layer of polypyrrole and poly (3-methylthiophene) were electrochemically deposited.

Chitosan (CS), derived by the alkaline deacetylation of chitin (Rinaudo, 2006), is insoluble in water in basic pH conditions because of its free amino groups; however, in acidic pH solutions, the amino groups can undergo a protonation process, thus making CS soluble. Properties such as biodegradability, low toxicity and good biocompatibility make CS suitable as a platform in biosensors. For CS fabrication, the electrogeneration approach

* Corresponding author. Tel./fax: +86 532 82898960.
E-mail addresses: zhangdun@ms.qdio.ac.cn, zhangdun@qdio.ac.cn (D. Zhang).

0956-5663/$ - see front matter © 2012 Elsevier B.V. All rights reserved.
http://dx.doi.org/10.1016/j.bios.2012.07.078

is simpler, more controllable, and more reproducible than the traditional dip-coating protocol. The electrogenerated film shows homogeneous morphology, which contributes to its improved performance in biological and chemical substance attachment, as well as biosensing stability (Wan et al., 2011a).

Sulfate-reducing bacteria (SRB) are anaerobic microorganisms that obtain their energy by reducing sulfate to sulfide (Muyzer and Stams, 2008), a highly corrosive and toxic substance. Therefore, SRB can be serious problems for industries and ecological systems (Wan et al., 2010b). Conventional methods for SRB detection, such as the most probable number (MPN) method (Abdelmalek and Rizk, 1958), involve a pre-enrichment or selective enrichment step followed by a biochemical test. However, the required complicated series of procedures can take up to 15 days to complete. A variety of other protocols have been reported for monitoring SRB populations, including improved MPN method (Stilinović and Hrenović, 2004; Vester and Ingvorsen, 1998), enzyme-linked immunosobent assays (Gibson and Gibson, 1988; Smith, 1982), biochemical tests (Louis et al., 1998), and molecular biotechniques (Cook et al., 2008; Lücker et al., 2007).

Electrochemical impedance spectroscopy (EIS), based on the response of an electrochemical cell to a small amplitude sinusoidal voltage signal as a function of frequency (Mamas, 2010), combines the information of both the resistive and capacitive properties of materials. An increasing trend towards the development of impedimetric biosensors is being observed. Impedimetric biosensors have been fabricated to study biomolecular reactions (Oliveira et al., 2008) as well as specific recognitions of proteins (Bogomolova et al., 2009), lectins (La Belle et al., 2007), antibodies (Rezaei et al., 2009), and nucleic acids (Hu et al., 2011). Our group has reported rapid and non-labeled impedimetric biosensors based on agglutination reaction (Wan et al., 2009) and antibody recognition platforms on 3D Ni foam substrates (Wan et al., 2010a), self-polymerized polydopamine films (Wan et al., 2011b), and RGSs-CS nanocomposite films (Wan et al., 2011a) for SRB detection.

In this study, we developed an impedimetric biosensor based on cell-mediated bioimprinted films for facile and rapid bacterial detection. SRB was selected as the template microorganism. A reduced graphene sheets (RGSs)/CS nanocomposite film was electrodeposited on the surface of an indium tin oxide (ITO) electrode, and the RGSs/CS hybrid film served as a substrate for SRB attachment. The RGSs were used to enhance the conductivity of the film and obtain good electrochemical signals for bacterial detection. After the absorption of bacteria on the RGSs-CS nanocomposite films, another layer of CS was electrodeposited around the immobilized pathogen. The bioimprinted bacteria were then washed away from the cell-mediated films by soaking in acetone. The binding of SRB was studied by analyzing the impedance change of the biosensor. The analytical performances of the bioimprinted impedimetric biosensor were also discussed.

2. Materials and methods

2.1. Chemicals and solutions

Natural graphite powder (99.99%) purchased from Beijing Chemical Company was used in RGSs synthesis. CS (95% deacetylation) was from Sinopharm Chemical Reagent Co., Ltd. (Shanghai, China). (Heptadecafluoro-1,1,2,2-tetradecyl) trimethoxysilane (HFTES, produced by Nanjing Daoning Chemical Co., Ltd.), a fluorinated silane coupling agent possessing a polyfluoroalkyl group, was used to reduce bacterial attachment on non-imprinted sites. Sodium nitrate, concentrated sulfuric acid, potassium permanganate, hydrogen peroxide, hydrazine, acetic acid, sodium hydrate, potassium ferricyanide, and potassium ferrocyanide were analytical grade and purchased from Sinopharm Chemical Reagent Co., Ltd. Magnesium sulfate, ammonium chloride, sodium sulphate, dipotassium hydrogen phosphate, calcium chloride, sodium hydroxide, sodium lactate, and yeast extract were used to prepare the modified Postgate's culture medium.

2.2. Bacterial cultivation

Seed bacteria were isolated from marine mud collected from the Bohai Sea, China. Pure SRB culture was grown in modified Postgate's medium for 4 days at 30 °C. Bacterial cells were isolated by centrifugation (6000 rpm, 20 min), and then rinsed twice with 0.2 M PBS (pH 7.4). The SRB culture was serially diluted with physiological saline solution, and the visible bacteria number was determined by the MPN method according to the American Society of Testing materials standard D4412-84. *Staphylococcus aureus*, *Micrococcus luteus*, *Vibrio anguillarum*, and *Vibrio alginolyticus* were used as control microorganisms.

2.3. Fabrication of the bioimprinted film

Graphene oxide (GO) was prepared from natural graphite according to the Hummers method (Hummers and Offeman, 1958). Graphite powder was oxidized to graphite oxide by concentrated H_2SO_4 and $KMnO_4$. Graphite oxide was then delaminated into GO sheets by sonication for 1 h. RGSs were obtained by reducing the GO sheets with hydrazine hydrate. In a typical procedure, 2 mL of 85% hydrazine hydrate was added to 100 mL of 1 mg mL^{-1} GO solution, and the reaction mixture was then heated at 120 °C for 12 h. Blank RGSs were obtained by filtration and drying in a vacuum.

A 1.0 wt% CS stock solution was prepared by dissolving CS flakes in 1% acetic acid solution at 40 °C. The pH of the stoke solution was adjusted to 6.0 with 1 M NaOH solution, and the solution was filtered and stored in a refrigerator (4 °C). The RGSs were suspended in CS solution at various concentrations (0–0.5 mg mL^{-1}).

The SRB-mediated bioimprinted film was fabricated as shown in Fig. 1. Before use, the ITO glass substrate was carefully cut into 1 cm × 1 cm pieces, and cleaned by sonication in ethanol and ultrapure water. The graphene-CS hybrid film was electrodeposited by immersing the ITO electrode in graphene-CS solution at a potential of −1.2 V. The template bacteria solution (10 μL, 1.0×10^7 cfu mL^{-1}) was added onto the surface of the RGSs-CS film and incubated for 2 h. Afterwards, the bioimprinting non-conductive CS film was electrogenerated around the adsorbed SRB in 1.0 wt% CS solution at −1.2 V for 30 s. After rinsing with deionized water, the electrode was transferred to 1.0 wt% fluorinated silane coupling solution. The coupling solution was freshly prepared with propanol and 1.0 wt% nitric acid, and stirred for 2 h to hydrolyze HFTES. Numerous studies have demonstrated that fluorinated coatings can inhibit bacterial adsorption (Aherne et al., 1996; Pasparakis and Alexander, 2007; Su et al., 2010). The electrode was immersed in acetone for 2 h to wash away the embedded SRB and remove any unbound fluorinated silane coupling agent. Finally, a series of bacteria solutions (10 μL) were added onto the surface of the bioimprinted electrode and incubated for 1 h for target bacterial detection. After each step, the electrode was rinsed thoroughly with deionized water. A non-imprinted film was prepared by the same procedure without the addition and adsorption of SRB templates.

2.4. Analytical procedures

Electrochemical measurements were performed with an electrochemical system (CHI 760C, CH instruments, Inc.) in a three-

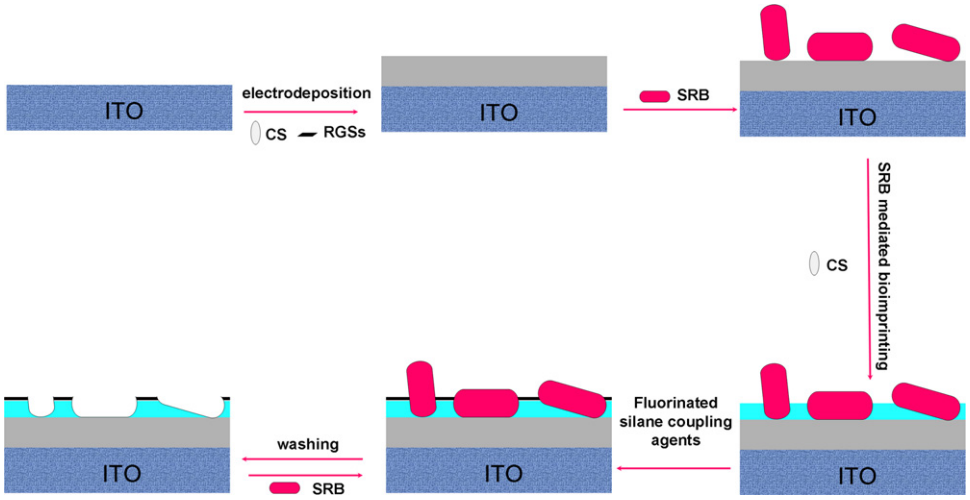

Fig. 1. Schematic diagram of fabrication procedure of bacteria-mediated bioimprinted films for bacterial detection.

electrode cell with functionalized ITO electrodes as working electrodes, an Ag/AgCl (3 M KCl) electrode as the reference electrode and a Pt wire as the counter electrode. The electrochemical properties of the RGSs-CS composite films were evaluated by cyclic voltammetry (CV). EIS was used to characterize the stepwise modification process of the functionalized electrodes and monitor the SRB population. Both CV and EIS measurements were performed in a 5 mM solution of redox couple $[Fe(CN)_6]^{4-/3-}$ prepared in 0.2 M PBS buffer (pH 7.4). The impedance spectra were recorded at the open circuit potential vs. Ag/AgCl (3 M KCl) and the amplitude of applied sinusoidal wave potential was 10 mV in the frequency range of 0.1–100 kHZ. The experiments were done in triplicate, and the means of the results were presented with the standard deviations.

3. Results and discussion

3.1. Synthesis and optimization of RGSs-CS film

RGSs were suspended in CS solution by sonication for 0.5 h. The carboxyl and hydroxyl groups of graphene can react with the active amino and hydroxyl functional groups of CS to form a well-dispersed RGSs-CS colloidal solution (Wan et al., 2011a). When the supplied potential was sufficient for the reduction of H^+ to H_2 on the cathode surface, the pH near the surface gradually increased. CS became insoluble at pH higher than 6.3 (Fernandes et al., 2003); consequently CS chains incorporated with RGSs were electrodeposited on the surface of the cathode.

The electrodeposition conditions, including graphene concentration, electrodeposition potential, and electrodeposition time, were optimized to obtain the RGSs-CS film with excellent electrochemical performance. The electrochemical properties of the composite films were evaluated by CV at a scan rate of 100 mV s^{-1} in 0.2 M PBS containing 5 mM $[Fe(CN)_6]^{4-/3-}$ redox probe. Fig. 2A shows the peak current changes of the RGSs-CS hybrid films obtained at different electrodeposition potentials. The electrochemical signals were very low and remained stable from −1.4 V to −1.3 V. A possible explanation for the unevenness and low conductivity of the films within this potential range was that the positively charged CS chains rapidly moved towards the cathode, and the combination between CS and the negatively charged RGSs was destroyed. When the potential was −1.2 V, the peak current signal reached 600 μA in the electrolyte containing 5 mM $[Fe(CN)_6]^{4-/3-}$, and the resulting films were smooth. Therefore, the optimized electrodeposition potential was −1.2 V.

The influence of the electrodeposition time on the electrochemical signals was investigated. Fig. 2B shows a relatively stable peak current signal from 240 s to 300 s. When the deposition time was long, the peak current responses decreased sharply. This result was due to the inhibition of electrodeposition by the accumulated H_2 around the cathode, which resulted in loose structures in the RGSs-CS films. Therefore, 300 s was chosen as the optimum electrodeposition time in subsequent experiments.

The concentration of graphene was also studied within the range of 0–0.5 mg mL^{-1}, and the results are shown in Fig. 2C. With increased graphene concentration from 0 mg mL^{-1} to 0.1 mg mL^{-1}, the peak current increased sharply due to the fascinating electrical conductivity of graphene. From 0.1 mg mL^{-1} to 0.5 mg mL^{-1}, the peak current changes were not very remarkable. The subtle changes in the peak current may have been caused by the differences of ITO substrate and manual cutting operation. At very high concentrations, it is difficult for the RGSs to bind chemically with CS, so the nanocomposite films electrodeposited on the surface of ITO electrodes became rough and unstable, which adversely affected the attachment of the SRB template. The graphene concentration of 0.3 mg mL^{-1} was selected in the fabrication of the conductive nanocomposite film because the peak current signal in this concentration was stable.

3.2. Fabrication of SRB-mediated bioimprinted film

EIS was used to characterize the stepwise modification process of the functionalized electrodes. Fig. 3 shows the Faradic impedance spectra for the redox of $[Fe(CN)_6]^{4-/3-}$ measured during the modification process of the ITO electrode. A modified Randles circuit with a constant phase element was used to simulate the experimental diagrams. In this equivalent circuit, R_s is the electrolytic resistance between the modified working electrode and the Ag/AgCl reference electrode, Q_{dl} is the double layer capacitance, Z_w is the Warburg impedance with a semi-infinite diffusion process, and R_{ct} is the charge transfer resistance of the $[Fe(CN)_6]^{4-/3-}$ redox probe. In Faradic impedance measurements, R_{ct} is the most sensitive parameter used to characterize the surface recognition process of the electrodes. When RGSs-CS nanocomposite film was deposited onto the ITO electrode, the R_{ct} decreased compared with the result obtained with bare ITO electrode because graphene facilitated the charge transfer process of $[Fe(CN)_6]^{4-/3-}$. A much larger resistance for the probe can be

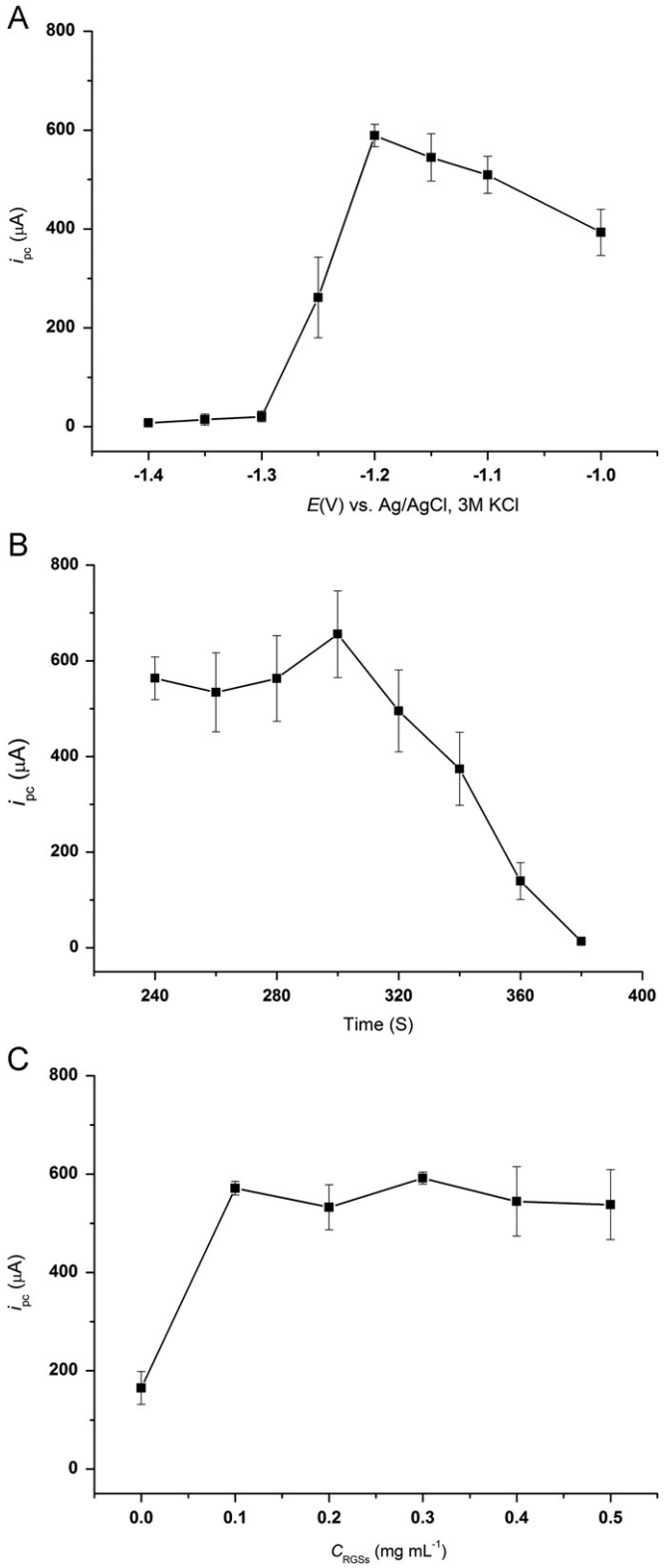

Fig. 2. Effects of electrodeposition potential (A), electrodeposition time (B), and RGSs concentration (C) on the peak current signal of conductive RGSs-CS hybrid films. The peak currents were obtained at the potential of −0.2 V from the CVs of RGSs-CS hybrid films in 0.2 M PBS containing 5 mM $[Fe(CN)_6]^{4-/3-}$ redox probe with a scan rate of 100 mV s^{-1}.

observed when SRB attached onto the conductive films because the bacteria hindered the charge transfer process. After the nonconductive CS film was formed to embed the bacteria, the

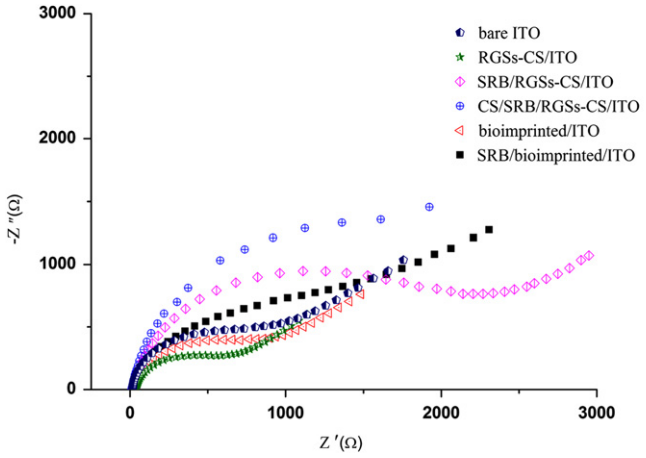

Fig. 3. Impedance spectra plots obtained with bare ITO electrode, RGSs-CS/ITO electrode, SRB/RGSs-CS/ITO electrode, CS/SRB/RGSs-CS/ITO electrode, and CS/SRB/RGSs-CS/ITO electrode after SRB removal, and SRB detection with the prepared bioimprinted electrode in PBS containing 5 mM $[Fe(CN)_6]^{4-/3-}$ as the probe. The concentration of SRB used for both attachment and detection was 1.0×10^7 cfu mL^{-1}. (Inert: the equivalent circuit used for simulating the results).

R_{ct} increased again. Subsequently, fluorine silane coupling agent was coated on the functionalized ITO electrode and the SRB were washed away by acetone to leave bioimprinted cavities. Consequently, the charge transfer resistance decreased sharply. Finally, the well bioimprinted electrode was used for SRB detection.

The morphological characteristics of the SRB-mediated bioimprinted films electrodeposited on ITO surfaces were examined by AFM, and the three-dimensional surface images are shown in Fig. 4. Fig. 4A shows the AFM image of the bioimprinted film after the electrodeposition of nonconductive CS. The bioimprinted film was uniform and the template bacteria were partly wrapped by a layer of nonconductive CS. The removal of bacterial templates was achieved by immersing the electrode in acetone, as described in the Section 2. Bioimprinted cavities were left on the surface of the films following SRB removal, as shown in Fig. 4B. The size of the recognition site was a little larger than the SRB templates because the structure was damaged during the washing procedure. These bioimprinted recognition sites can selectively bind with bacteria based on differences in size and shape.

3.3. Selectivity of the bacteria-mediated bioimprinted film

To evaluate the selectivity of the bacteria-mediated bioimprinted film, four kinds of bacteria, *M. luteus*, *S. aureus*, *V. anguillarum* and *V. alginolyticus*, have been chosen to perform control experiments. *S. aureus* and *M. luteus* are small round cocci forming clusters or spherical shape, while *V. anguillarum* and *V. alginolyticus* have a curved rod shape (comma shape). The concentrations of SRB and the control bacteria were 1.0×10^8 cfu mL^{-1}. Bacterial suspensions were added to the films and incubated for 1 h, and EIS measurements were performed in 0.2 M PBS containing 5 mM $[Fe(CN)_6]^{4-/3-}$. The impedance spectra were obtained and are shown in Fig. 5A. Fig. 5B shows the R_{ct} changes (ΔR_{ct}) obtained before and after adding the five kinds of bacteria to bioimprinted ITO electrode. The R_{ct} change after SRB attachment was more remarkable than those caused by the other bacteria, and ΔR_{ct} value reached 434.5 Ω with the relative deviation standard (RSD) of 4.7%. Moreover, compared with the two cocci, *V. anguillarum* and *V. alginolyticus* have greater influence on the electrochemical signal. This is because *V. anguillarum* and *V. alginolyticus* have relatively similar shape and size as SRB, so they would be trapped easier by the bioimprinted cavities. These results illustrated that the impedimetric biosensor based on

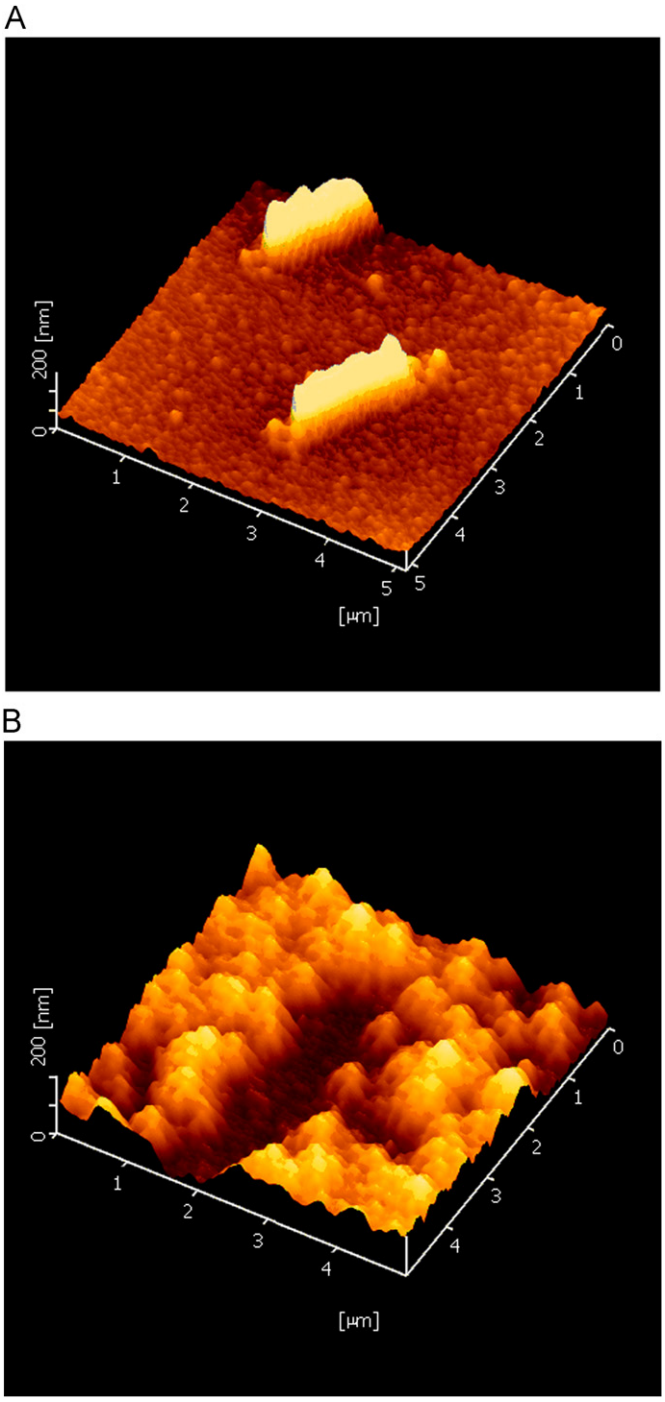

Fig. 4. AFM images of the SRB-mediated film before (a) and after (b) the template removal. The concentration of SRB used for attachment was 1.0×10^7 cfu mL^{-1}.

bacteria-mediated bioimprinted films showed good shape and size selectivity.

3.4. Bacterial detection

To determine the relationship between ΔR_{ct} values and the concentrations of SRB, the bacteria-mediated bioimprinted electrode was exposed to various SRB concentrations from 1.0×10^0 cfu mL^{-1} to 1.0×10^8 cfu mL^{-1}. The Nyquist plots obtained are shown in Fig. 6A. The diameter of the Nyquist circle increased with increased SRB concentrations from 1.0×10^4 cfu mL^{-1} to 1.0×10^8 cfu mL^{-1}. The calibration curves of the SRB bioimprinted and non-bioimprinted

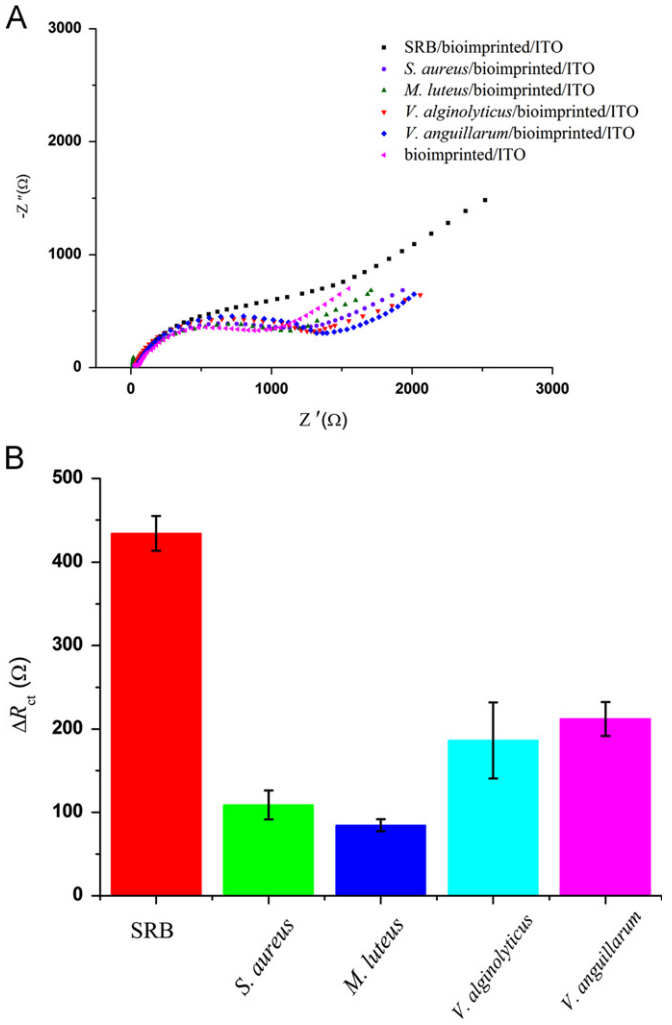

Fig. 5. Impedance spectra obtained with bioimprinted sensor and the biosensor after incubated with 1.0×10^8 cfu mL^{-1} SRB, *S. aureus*, *M. luteus*, *V. anguillarum*, and *V. alginolyticus* in PBS containing 5 mM $[Fe(CN)_6]^{4-/3-}$ as the probe (A). The comparison of R_{ct} changes of the impedimetric biosensor based on SRB-mediated bioimprinted film to SRB, *S. aureus*, *M. luteus*, *V. anguillarum*, and *V. alginolyticus* (B). ΔR_{ct} is the change of charge transfer resistance of impedimetric sensor before and after incubation with different bacteria.

sensors are shown in Fig. 6B. A linear relationship between ΔR_{ct} values and the logarithm of bacterial concentration was obtained with the bioimprinted electrodes for concentrations ranging from 1.0×10^4 cfu mL^{-1} to 1.0×10^8 cfu mL^{-1}, with a correlation coefficient of 0.98. The RSD were 16.01%, 15.06%, 14.26%, 7.39%, and 8.73% for 1.0×10^4, 1.0×10^5, 1.0×10^6, 1.0×10^7, and 1.0×10^8 cfu mL^{-1} SRB, respectively. The regression equation is $\Delta R_{ct} = 106.09 \log N_{SRB} - 402.63$ with a detection limit of 0.7×10^4 cfu mL^{-1} at a signal to noise ratio of 3δ (where δ is the standard deviation of a blank solution). Compared with bioimprinted sensors, the non-bioimprinted electrodes have lower sensitivity for SRB detection. Hence, the impedimetric biosensor based on bacteria-mediated bioimprinted films in this work can be used in bacterial detection.

The selectivity of a biosensor depends almost solely on the recognition element, since different recognizing elements account for varied degrees of selectivity. For example, monoclonal antibodies can be used to immunotrap target bacteria from different bacterial genera by specific antigen/antibody interactions (Karoonuthaisiri et al., 2009; Wan et al., 2011a,b). Lectins can recognize bacteria or fungi by selectively and reversibly integrating with the typical carbohydrate structures in the cell membrane (Shen et al., 2007). Some classes of antibiotics can discriminate

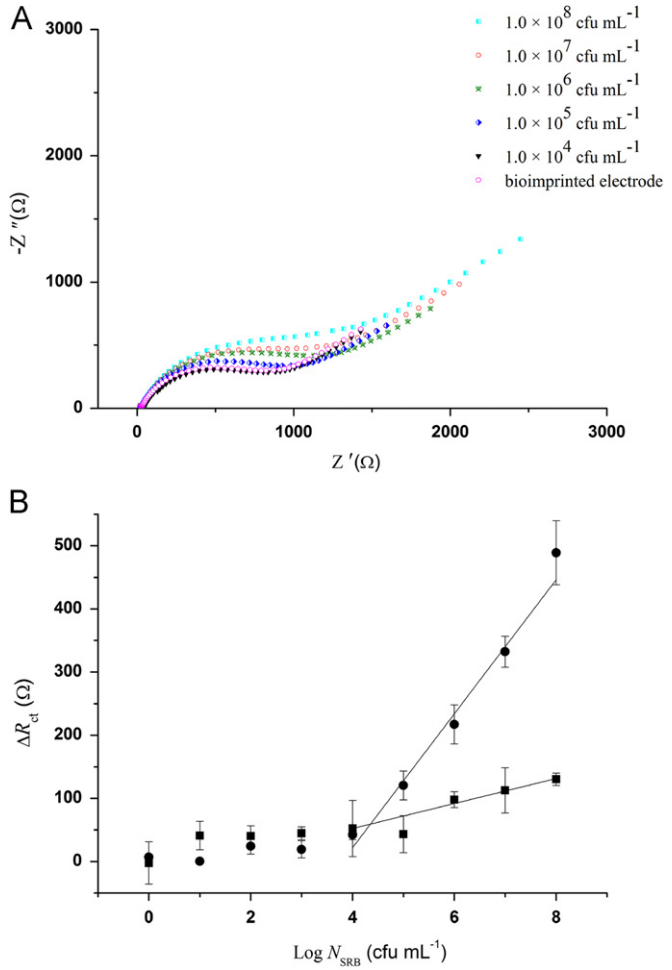

Fig. 6. Nyquist plots of the bioimprinted electrode and the electrode after exposing to various concentrations of SRB: 1.0×10^4 cfu mL^{-1}, 1.0×10^5 cfu mL^{-1}, 1.0×10^6 cfu mL^{-1}, 1.0×10^7 cfu mL^{-1}, and 1.0×10^8 cfu mL^{-1} (A) and calibration curve for the detection of SRB with bioimprinted (●) and non-imprinted (■) electrodes (B). ΔR_{ct} is the change of charge transfer resistance of impedimetric sensor before and after incubation with different concentrations of SRB.

between Gram-positive and Gram-negative bacteria by the structural differences of bacterial cell walls (Gu et al., 2003a,b). Aptamers, specific nucleic acid sequences, can bind target microorganisms with high affinity and specificity (Torres-Chavolla and Alocilja, 2009) because the aptamers are selected by an *in vitro* SELEX (systematic evolution of ligands by exponential enrichment) process. In the present work, the bioimprinted film can recognize bacteria based on differences in shape and size. Compared with the bioimprinted films, biological bio-recognition elements, such as antibiotics, lectins, antibodies, and aptamers, are inherently 'fragile'. In other words, their activity is easily lost if not stored or used properly. At extreme conditions, the biological structures of these bio-recognition elements would be damaged, leading to the vanishing of specific binding abilities. Another advantage for the films is that the fabrication processes for bioimprinted films are facile and controllable, and the materials used are biodegradable, lowly toxic, biocompatible, and low cost.

4. Conclusion

In summary, a low-cost, versatile, and rapid impedimetric biosensor based on the bacteria-mediated bioimprinting technique has been fabricated for bacterial detection. Marine microorganism SRB have been chosen as the template bacteria. RGSs-CS composite film has been fabricated for bacterial attachment, and a layer of CS nonconductive film has been electrodeposited to wrap the pathogen. The proposed sensor shows good selectivity based on size and shape differences. The selectivity and accuracy for bacterial detection can be improved if the bioimprinting technique is used together with other bio-recognition elements, such as antibodies, antibiotics, lectins, and aptamers. This research holds great promise for the development of electrochemical biosensors for bacterial detection based on bioimprinted films.

Acknowledgments

This work was supported by the National Natural Science Foundation of China (Grant No. 41076047) and the Shandong Provincial Natural Science Foundation, China (Grant No. ZR2010DM004).

References

Abdelmalek, Y., Rizk, S.G., 1958. Nature 182 (4634). (538–538).
Aherne, A., Alexander, C., Payne, M.J., Perez, N., Vulfson, E.N., 1996. Journal of the American Chemical Society 118 (36), 8771–8772.
Bogomolova, A., Komarova, E., Reber, K., Gerasimov, T., Yavuz, O., Bhatt, S., Aldissi, M., 2009. Analytical Chemistry 81 (10), 3944–3949.
Bolisay, L.D., Culver, J.N., Kofinas, P., 2006. Biomaterials 27 (22), 4165–4168.
Chen, L., Xu, S., Li, J., 2011. Chemical Society Reviews 40 (5), 2922–2942.
Cheng, Z., Wang, E., Yang, X., 2001. Biosensors & Bioelectronics 16 (3), 179–185.
Cook, K.L., Whitehead, T.R., Spence, C., Cotta, M.A., 2008. Anaerobe 14 (3), 172–180.
Dickert, F.L., Hayden, O., 2002. Analytical Chemistry 74 (6), 1302–1306.
Fernandes, R., Wu, L.Q., Chen, T.H., Yi, H.M., Rubloff, G.W., Ghodssi, R., Bentley, W.E., Payne, G.F., 2003. Langmuir 19 (10), 4058–4062.
Gibson, S.A.W., Gibson, G.R., 1988. Letters in Applied Microbiology 7 (2), 33–35.
Gu, H., Ho, P., Tong, E., Wang, L., Xu, B., 2003a. Nano Letters 3 (9), 1261–1263.
Gu, H., Ho, P., Tsang, K., Wang, L., Xu, B., 2003b. Journal of the American Chemical Society 125 (51), 15702–15703.
Haupt, K., Mosbach, K., 2000. Chemical Reviews 100 (7), 2495–2504.
Hayden, O., Dickert, F.L., 2001. Advanced Materials 13 (19), 1480–1483.
Hayden, O., Bindeus, R., Haderspock, C., Mann, K.J., Wirl, B., Dickert, F.L., 2003. Sensors and Actuators B 91 (1–3), 316–319.
Hayden, O., Lieberzeit, P.A., Blaas, D., Dickert, F.L., 2006. Advanced Functional Materials 16 (10), 1269–1278.
Hong, C.-C., Chang, P.-H., Lin, C.-C., Hong, C.-L., 2010. Biosensors & Bioelectronics 25 (9), 2058–2064.
Hu, Y., Hua, S., Li, F., Jiang, Y., Bai, X., Li, D., Niu, L., 2011. Biosensors & Bioelectronics 26 (11), 4355–4361.
Hummers, W.S., Offeman, R.E., 1958. Journal of the American Chemical Society 80 (6) 1339–1339.
Karoonuthaisiri, N., Charlermroj, R., Uawisetwathana, U., Luxananil, P., Kirtikara, K., Gajanandana, O., 2009. Biosensors & Bioelectronics 24 (6), 1641–1648.
La Belle, J.T., Gerlach, J.Q., Svarovsky, S., Joshi, L., 2007. Analytical Chemistry 79 (18), 6959–6964.
Li, X., Husson, S.M., 2006. Biosensors & Bioelectronics 22 (3), 336–348.
Louis, D., Sorlier, P., Wallach, J., 1998. Clinical Chemistry and Laboratory Medicine 36 (5), 295–298.
Lücker, S., Steger, D., Kjeldsen, K.U., MacGregor, B.J., Wagner, M., Loy, A., 2007. Journal of Microbiological Methods 69 (3), 523–528.
Mamas, I.P., 2010. Electrochimica Acta 55 (14), 4227–4233.
Manju, S., Hari, P.R., Sreenivasan, K., 2010. Biosensors & Bioelectronics 26 (2), 894–897.
Mazzotta, E., Picca, R.A., Malitesta, C., Piletsky, S.A., Piletska, E.V., 2008. Biosensors & Bioelectronics 23 (7), 1152–1156.
Muyzer, G., Stams, A.J.M., 2008. Nature Reviews Microbiology 6 (6), 441–454.
Namvar, A., Warriner, K., 2007. Biosensors & Bioelectronics 22 (9–10), 2018–2024.
Oliveira, M.D.L., Correia, M.T.S., Coelho, L.C.B.B., Diniz, F.B., 2008. Colloids and Surfaces B 66 (1), 13–19.
Özcan, A.A., Say, R., Denizli, A., Ersöz, A., 2006. Analytical Chemistry 78 (20), 7253–7258.
Pasparakis, G., Alexander, C., 2007. Analyst 132 (11), 1075–1082.
Rezaei, B., Khayamian, T., Majidi, N., Rahmani, H., 2009. Biosensors & Bioelectronics 25 (2), 395–399.
Rinaudo, M., 2006. Progress in Polymer Science 31 (7), 603–632.
Shen, Z., Huang, M., Xiao, C., Zhang, Y., Zeng, X., Wang, P., 2007. Analytical Chemistry 79 (6), 2312–2319.
Smith, A.D., 1982. Archives of Microbiology 133 (2), 118–121.
Stilinović, B., Hrenović, J., 2004. Folia Microbiologica 49 (5), 513–518.

Su, X.J., Zhao, Q., Wang, S., Bendavid, A., 2010. Surface and Coatings Technology 204 (15), 2454–2458.
Syu, M.-J., Chiu, T.-C., Lai, C.-Y., Chang, Y.-S., 2006. Biosensors & Bioelectronics 22 (4), 550–557.
Thoelen, R., et al., 2008. Biosensors & Bioelectronics 23 (6), 913–918.
Torres-Chavolla, E., Alocilja, E., 2009. Biosensors & Bioelectronics 24 (11), 3175–3182.
Vester, F., Ingvorsen, K., 1998. Applied and Environmental Microbiology 64 (5), 1700–1707.
Wan, Y., Zhang, D., Hou, B., 2009. Talanta 80 (1), 218–223.
Wan, Y., Zhang, D., Wang, Y., Hou, B., 2010a. Electrochemistry Communications 12 (2), 288–291.
Wan, Y., Zhang, D., Liu, H., Li, Y., Hou, B., 2010b. Electrochimica Acta 55 (5), 1528–1534.
Wan, Y., Lin, Z., Zhang, D., Wang, Y., Hou, B., 2011a. Biosensors & Bioelectronics 26 (5), 1959–1964.
Wan, Y., Zhang, D., Wang, Y., Qi, P., Hou, B., 2011b. Biosensors & Bioelectronics 26 (5), 2595–2600.